CHEMISTRY OF MATERIALS

pubs.acs.org/cm

Article

Caged Colloids

Zhe Xu, Theodore Hueckel, William T. M. Irvine, and Stefano Sacanna*

Cite This: *Chem. Mater.* 2023, 35, 6357−6363

Read Online

ACCESS | Metrics & More | Article Recommendations | Supporting Information

ABSTRACT: Colloidal microcontainers, such as hollow capsules and colloidosomes, have a range of applications, including drug delivery, energy storage, and artificial protocells. In this study, we present a versatile and scalable self-assembly approach for encapsulating cargo particles within well-defined porous membranes or cages. The encapsulation process involves camouflaging cargo within a liquid matrix that serves as a scaffold for satellite particles to form densely packed shells around. These satellites fuse to create self-standing cages, after which the liquid matrix is dissolved, trapping the cargo inside. By adjusting the fusion protocol, we can control the porosity of the cages at various length scales. We demonstrate the potential of this technique by employing functional cargo to showcase transmembrane transport phenomena, such as the delivery and active uptake of nanoparticles.

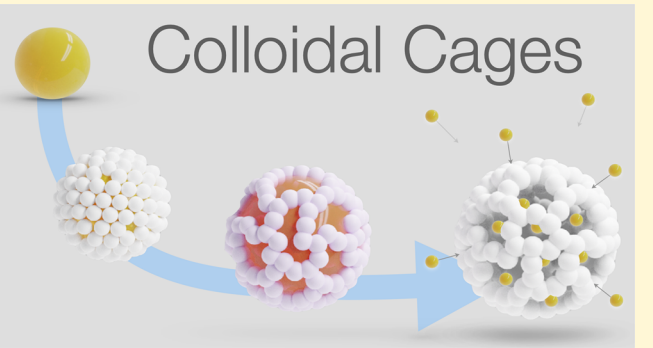

INTRODUCTION

Impossible bottles, exemplified by the iconic "ship-in-a-bottle", are containers with openings too small for their contents to exit. Microscopic versions of these containers can exhibit emergent host−guest functionality, as seen in cellular nuclei.[1] Here, vital DNA cargo is encapsulated by porous nuclear membranes, controlling molecular transport for cellular communication and maintaining a secure environment. Creating such microscopic structures presents a significant synthetic challenge, which necessitates control over container morphology and the positioning of contents within.

In this work, we present a versatile synthetic route for colloidal impossible bottles, wherein we encapsulate nonspecific cargo into containers with adjustable porosity in a consistent and scalable manner. Our approach centers on constructing a colloidosome structure that encapsulates the selected cargo material.[2,3] Colloidosomes feature membranes composed of densely packed shell particles, with the interstitial spaces between them forming well-defined pores.[4−7]

The conventional method of particle membrane formation, Pickering emulsification, involves generating liquid droplets that serve as soft templates for satellite particles to organize around.[8−10] While under ideal conditions, Pickering emulsification can produce droplets with uniform sizes, practical issues such as the influence of particle concentration, particle wettability, oil/water ratio, and shear forces can contribute to polydispersity in droplet sizes. This, in turn, can lead to nonuniform colloidosome sizes and inconsistent cargo loads, thereby posing potential limitations to its effectiveness.[11]

As an alternative, microfluidic techniques can be employed to create more regular and controlled colloidosome structures.[12,13] These methods allow for precise manipulation of droplet size and satellite particle organization, resulting in a higher degree of uniformity in both colloidosome size and cargo load. Despite these advantages, microfluidic techniques involve the sequential synthesis of particles, rendering them unsuitable for large-scale production.

A less commonly utilized soft-template strategy involves the heteroaggregation of two well-defined building blocks: monodispersed emulsion droplets and solid satellite particles.[14] This approach leads to the formation of hybrid clusters, in which the droplets serve as both uniform templates and vehicles for carrying discrete cargo into the final colloidosome structure. By employing this method, we can create more controlled and consistent colloidosomes, overcoming the limitations of traditional techniques.

The primary engineering challenge in this approach lies in the formation of uniform satellite monolayers on the soft emulsion droplet cores. Achieving this uniformity is crucial for the successful development of well-defined porous structures, ensuring consistent cargo encapsulation and effective utilization of the colloidosomes in various applications.

To accomplish this objective, we leverage polymer-mediated interactions between polymer-coated oil droplets and polymer-free satellite particles.[15] The assembly process begins when the

Received: May 4, 2023
Revised: June 10, 2023
Published: June 26, 2023

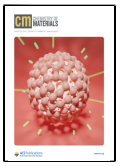

https://doi.org/10.1021/acs.chemmater.3c01053
Chem. Mater. 2023, 35, 6357−6363

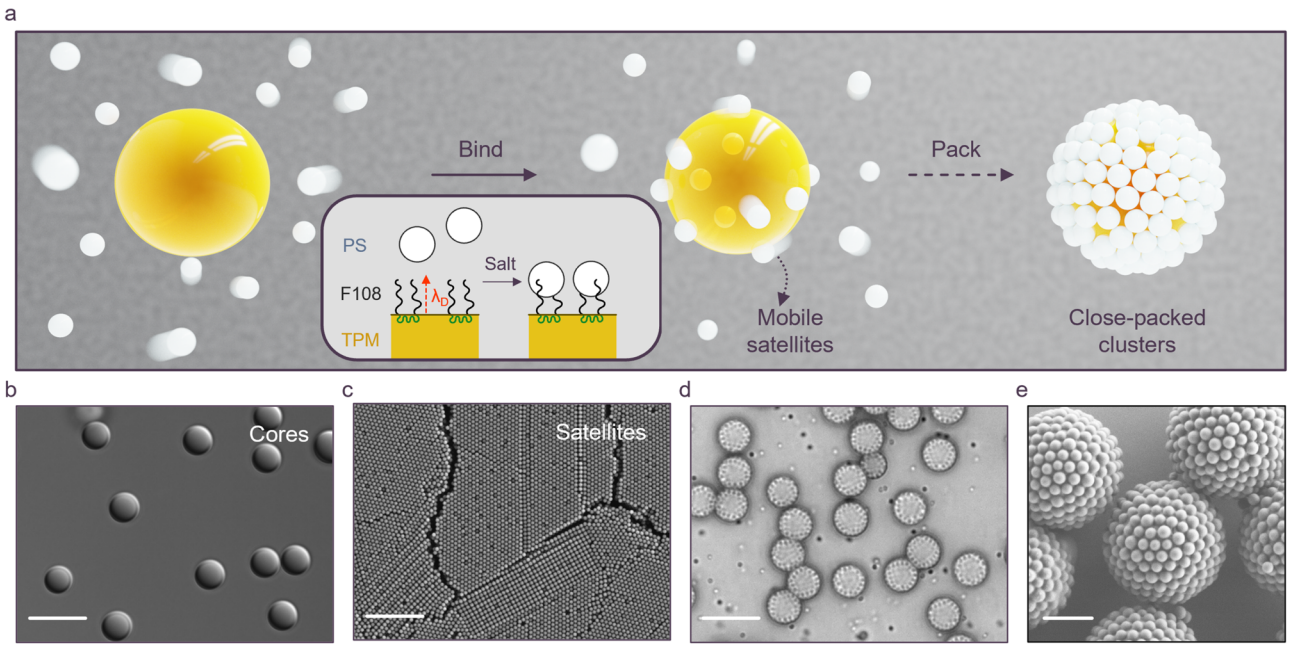

Figure 1. Polymer-adsorption based heteroaggregation. (a) Schematic representation of the system. F108-coated TPM core droplets (*yellow*) capture bare satellite PS particles (*white*) when the Debye length (λ_d) is screened. Satellite mobility on the fluid interface leads to close-packed clusters. (b) Optical image of TPM oil droplet. (c) SEM image of solid PS satellites. (d, e) Optical and SEM images of solidified clusters exhibiting close-packed satellites. Scale bars for (b)−(d) are 5 μm. Scale bar for (e) is 2 μm.

polymer brush on the droplet's surface makes contact with the satellite particles, initiating adsorption and effectively bridging their surfaces together.

The polymer brush's mobility at the oil−water interface plays a crucial role in this process, as it enables the bonded satellite particles to rearrange and achieve densely packed configurations around the droplet core. This reconfiguration helps create a more uniform satellite monolayer on the soft core, ensuring the formation of well-defined porous structures.

Once the satellite particles are optimally positioned, they are permanently fused together to form a solid shell. At this stage, the core template, which consists of the polymer-coated oil droplets, is dissolved, leaving behind self-standing cages loaded with the desired cargo.

RESULTS AND DISCUSSIONS

Formation of Hybrid Clusters through Polymer Adsorption. To create stable cages from hybrid clusters, satellite particles need to be densely packed around the cores and securely connected. However, heteroaggregation often leads to uneven core coatings due to the limited mobility of attached satellites.[16−18] Although reconfigurable interactions can be achieved through advanced surface chemistry,[19−21] a more scalable and versatile method is desirable. In our approach, particle shells are formed similarly to Pickering emulsions, where the mobility of satellites on a liquid interface enables structural reconfiguration, leading to densely packed crystalline arrangements (Figure 1a).

In our system, the liquid core consists of 3-(trimethoxysilyl)-propyl methacrylate (TPM), which is known for forming well-defined emulsion droplets through a two-stage hydrolysis−condensation process[22] (Figure 1b).

To create a targeted core−satellite attraction, we decorate TPM droplets with the block copolymer Pluronic F108, which mediates colloidal interactions through polymer bridging.[15] As illustrated in Figure 1, hybrid clusters form when polymer-coated TPM cores are introduced to a concentrated suspension of polymer-free polystyrene (PS) satellites in the presence of NaCl. The salt reduces the Debye screening length of the system, allowing cores and satellites to come into contact and form polymer bridges. An excess of satellites in the mixture is necessary to minimize the likelihood of TPM cores binding together through shared satellites.

Typically, heteroaggregation can be driven by van der Waals forces or electrostatic attraction between oppositely charged species without the need for polymer bridges. However, in our system, using like-charged building blocks is essential to avoid excessive wetting of TPM on satellites, which often results in disordered multilayered clusters (see Figure S1).

A unique feature of TPM cores is their capacity to harden on demand through photoinitiated polymerization. As demonstrated in Figure 1e, the polymerization process allows us to image dry clusters via electron microscopy and obtain valuable information on their shell structure. Specifically, we can examine how experimental conditions affect wetting (Figures S2 and S3), satellite density bound to the core, and the presence of defects in the final shell.

To incorporate payload into the clusters, we leverage another beneficial property of TPM: its ability to condense on a wide range of materials. We allow TPM droplets to form in the presence of suspended cargo particles, which act as nuclei. This results in the heterogeneous nucleation of TPM, yielding hybrid emulsion droplets uniformly loaded with cargo material.[23]

The combined effect of this heterogeneous nucleation process and the nonspecific polymer-mediated interactions that link cores and satellites results in a versatile assembly toolkit. This toolkit can be employed to prototype a diverse range of hybrid clusters. In our experiments, we explored

https://doi.org/10.1021/acs.chemmater.3c01053
Chem. Mater. 2023, 35, 6357−6363

various shell and core sizes, as well as different contents embedded within the TPM core (Figure 2).

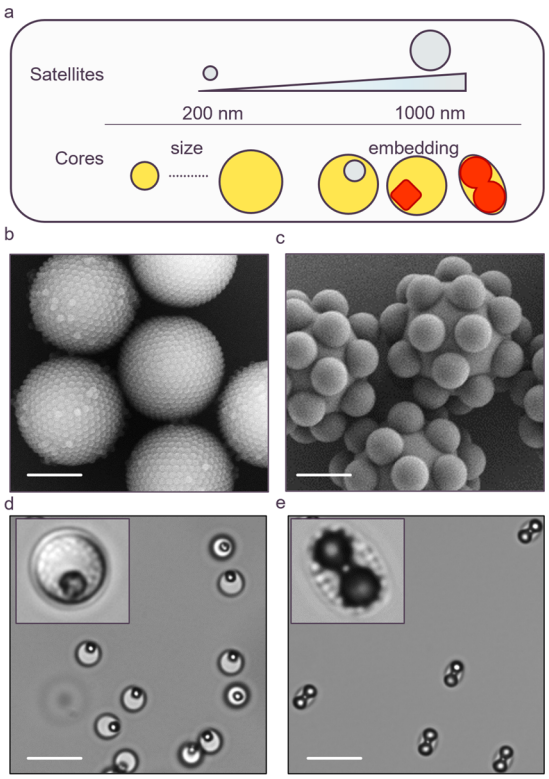

Figure 2. Scope of clustering strategy. (a) Satellite and core sizes can be adjusted without compromising the strategy's viability. Colloidal cargoes of various shapes or materials can be embedded by growing TPM around their surface through heterogeneous nucleation. (b) Clusters with low satellite/core size ratio about 0.05 display minimal defects. (c) Visible packing imperfection and strains are observed for high satellite/core size ratio about 0.15. (d) Small cube-shaped hematite particles show no geometric distortion on the TPM droplet. Inset: satellites are seen packed around the cargo loaded core. (e) Large peanut-shaped hematite particles cause TPM to adapt to the local curvature and form ellipsoidal droplets. Scale bars for (b) and (c) are 1 μm. Scale bars for (d)−(e) are 6 μm.

Satellite Fusion and Colloidal Cages. The bonding between coordinated satellites must be established chemically or physically before the soft liquid TPM template can be safely removed without compromising the colloidosome structure. Various methods of securing satellites have been reported in literature, such as chemical cross-linking, bioconjugation, *in situ* gelation, and polymerization.[24]

In this study, we use PS satellites that undergo a glass transition at room temperature in the presence of an organic solvent, providing a convenient method to adhere satellites into a continuous, robust shell. Dichloromethane (DCM) is chosen for its excellent miscibility with PS and its low boiling point, which allows for quick and easy post-treatment removal. The fixed shells are treated with ethanol to selectively dissolve the TPM core, revealing the caged cargo material (Figure 3a,b).

Along with the satellite fusion process, DCM also swells the TPM core, leading to the development of fissures on the surface as the packing density effectively drops. The average size of the fissures increases over time for tunable porosity

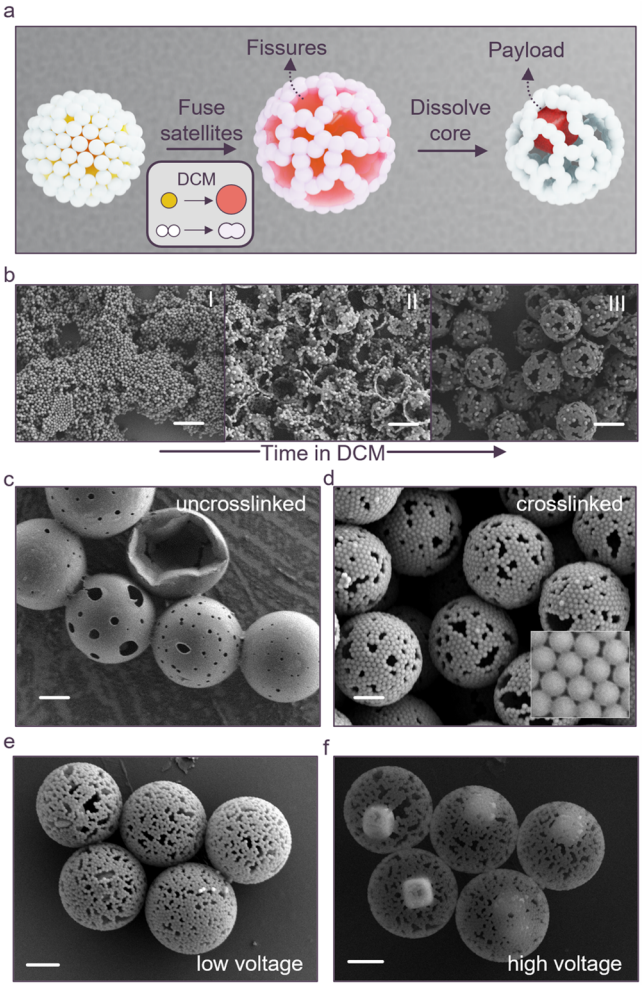

Figure 3. Cage fusion. (a) Schematic illustration of transforming close-packed clusters into caged structures by fusing satellites with DCM and dissolving the soft template (TPM core). Swelling of the liquid core leads to open fissures on the surface. Colloidal cargo is locked inside due to relatively small porosity. (b) Structural evolution of cages over time in DCM (I–III: 1, 5, and 10 s, respectively). Self-standing colloidosome membranes emerge due to stronger physical bonding among satellites. Scale bars: 3 μm. (c, d) Comparative analysis between uncrosslinked PS satellites and DVB-cross-linked PS indicates that the former deforms nearly instantaneously, faster than the 10-s exposure to DCM, thus forming a film. In contrast, cross-linked PS deforms at a slower rate, permitting individual particles to partially interpenetrate while primarily maintaining their shape. Inset in (d) shows open interstitial pores. (e, f) Electron microscope imaging at low and high voltage respectively emphasizes both the membrane structure and embedded cargo. Scale bars for (c)−(f): 1 μm.

(Figure 3a), and removal of the DCM preserves the fissure pattern.

In Figure 3c,d, we demonstrate how the choice of satellite can influence porosity. For instance, uncrosslinked PS satellites fully merge in DCM, closing interstitial spaces and leaving only large fissures open. Conversely, PS satellites cross-linked with divinylbenzene (DVB) maintain their spherical shape, resulting in two levels of porosity: the small gaps between close-packed satellites and larger fissures.

After core dissolution, SEM images reveal free-standing cages containing cargo, with the cargo being too large to

https://doi.org/10.1021/acs.chemmater.3c01053
Chem. Mater. 2023, 35, 6357−6363

escape through the fissures created during satellite fusion (Figures 3e,f and S5−7).

Fissure formation is a direct consequence of the core surface expansion while the number of attached satellites remains constant. To reduce or prevent fissures, an overpacked state can be achieved by shrinking the core before fusing satellites (Figure 4c).

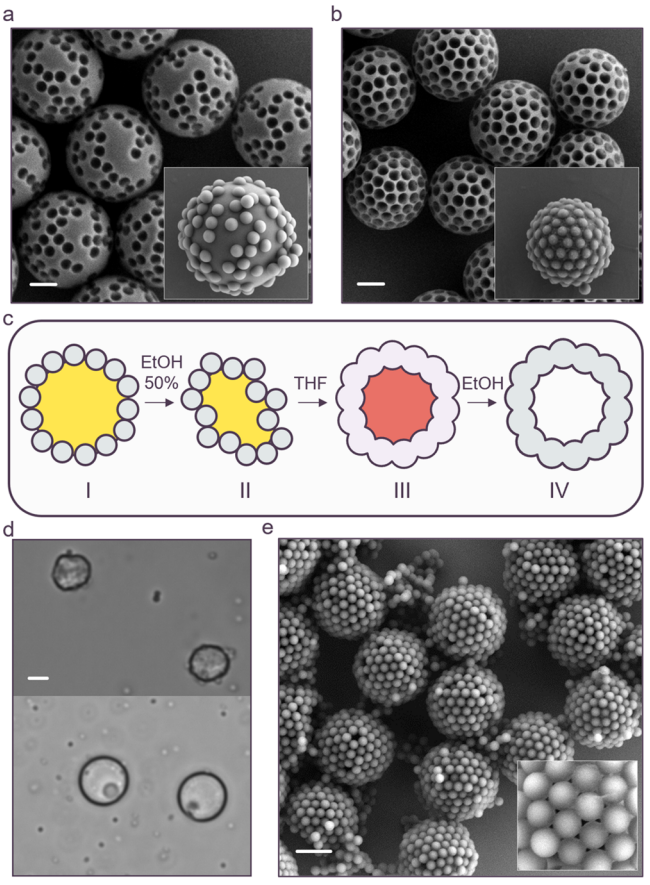

Figure 4. Shrink-packing. (a, b) Dimple analysis before and after ethanol treatment. Insets display clusters prior to satellites removal. (c) Schematic representation of shrink-packing process: I → II, shrinkage of liquid core with ethanol leads to overpacked nonspherical cluster; II → III, swelling with THF compensates the volume loss and restores spherical close-packing while fusing satellites together; III → IV, dissolution of core yields fissure-free cages. (d) Optical image of stages II (*top*) and III (*bottom*). (e) SEM image of uniform product IV with inset showing open interstices. All scale bars: 1 μm.

While high ethanol concentrations can completely dissolve TPM cores, lower ethanol concentrations cause core shrinkage and a subsequent increase in packing density. For example, treating sparsely coated clusters (Figure 4a) with 50% ethanol results in a close-packed state (Figure 4b) as cores shrink and satellites remain attached.

In clusters that are already well-packed, a shrinking core causes a buckling event since the cores can no longer accommodate the same number of satellites while maintaining a spherical shape. The crumpled clusters regain their spherical form when swollen in organic solvent, with the satellites fusing simultaneously (Figure 4d).

The resulting caged structures are free of fissures, and pores consist solely of interstices between satellites (Figure 4e).

Depending on the cargo size and cage porosity, contents can be retained indefinitely, released on demand, or initiate local chemical reactions in response to various stimuli.

For example, hematite cargo can be selectively etched in the presence of acid to produce iron(III) ions capable of diffusing through pores, while the hematite remains confined within the cage (Figures 5a and S8). A range of other cargos may be similarly released under different stimuli, creating local chemical sources to power specific reactions or release drugs via prefilled nanoporous cargo.[25,26]

Cargo can also serve as a driving force to actively fill cages with species small enough to pass through the pores.[27] Hematite cargo catalytically breaks down hydrogen peroxide when exposed to light, generating a gradient around the particle which attracts tracer particles through diffusiophoresis[28,29] (Figure 5b). Upon illumination, tracer particles smaller than the average pore size are observed gathering inside the capsule, as evidenced by a bright fluorescent signal. As soon as the light is turned off, some tracers are seen diffusing out of the pores. However, tracers can also be trapped for an extended period after the light is switched off due to entropic bottling[30,31] (see Supplementary Video 1), effectively disrupting the concentration equilibrium. In this example, a simple accumulation and delivery process is illustrated, though more intricate colloidosomes with stimuli-responsive pores[25,32−35] could potentially transport cargo back and forth to actively communicate with one another.

CONCLUSIONS

In summary, our findings demonstrate a versatile assembly approach for constructing monodisperse colloidal cages from the bottom up, with diverse functional cargo securely enclosed. The robust nature of polymer-mediated interactions and their effectiveness in heteroaggregating various particles and TPM droplets into uniform close-packed clusters pave the way for designing stimuli-responsive colloids with transferable contents. By integrating the entropic bottling effect of porous cages with active uptake, functional colloidal membranes can be engineered to simulate active transport in cells and offer on-demand delivery at larger scales for the investigation of cooperative colloidal behaviors.

METHODS

Satellite Particles. Monodisperse polystyrene spheres with a diameter of approximately 250 nm are produced using surfactant-free emulsion polymerization, incorporating a trace amount of divinylbenzene (DVB) as a cross-linker. In a typical synthesis, 10 mL of styrene monomer and 25 μL of DVB oil are combined with 500 mL of deionized water in a 1 L three-neck round-bottom flask. The system is purged with nitrogen for 30 min while stirring at 330 rpm. The temperature is then raised to 60 °C, and 0.75 g of potassium persulfate dissolved in 20 mL of deionized water is quickly injected into the flask. The reaction mixture is allowed to proceed overnight, after which the resulting product is washed three times with deionized water through a centrifugation and resuspension process. This protocol yields negatively charged particles with a typical zeta potential of −60 mV at neutral pH (Malvern Zetasizer NanoS). The size and cross-linking density of the synthesized particles can be adjusted by modifying the initial concentrations of styrene and DVB. The optimal DVB-to-styrene volume ratio, determined empirically, ranges from 0.15% to 0.25%. Polystyrene spheres of larger size, as utilized in Figure S3, were obtained via repeated seeded growth method, employing the above protocol iteratively until the desired dimension was reached.

https://doi.org/10.1021/acs.chemmater.3c01053
Chem. Mater. 2023, 35, 6357−6363

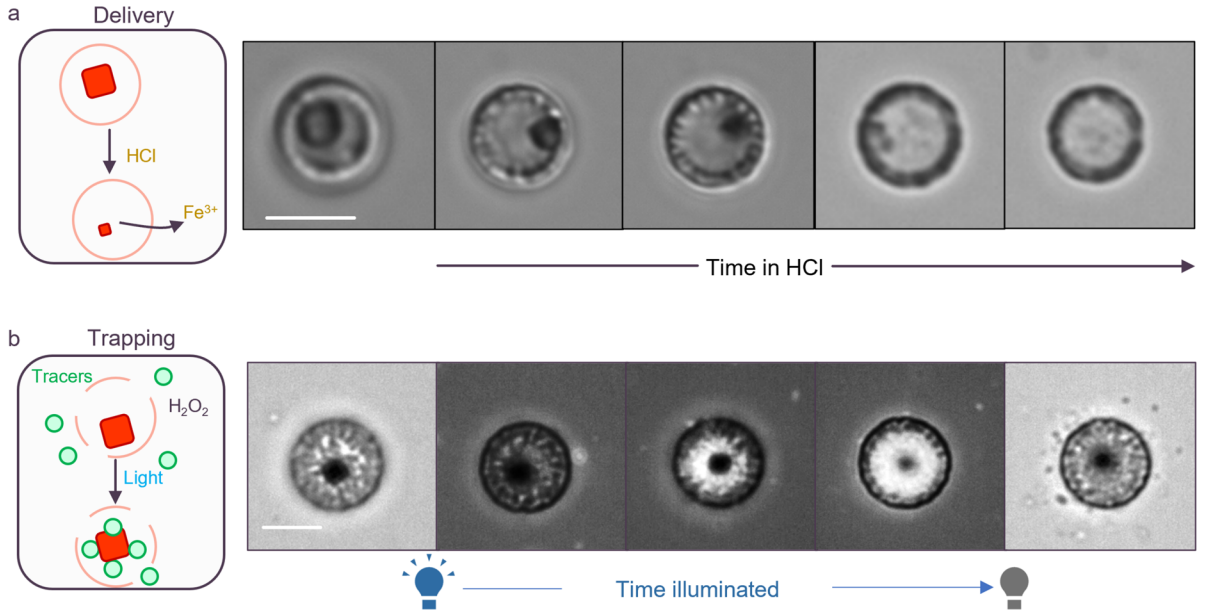

Figure 5. Active Transmembrane Transport. (a) Hematite cargo delivery into the surrounding is achieved by selective etching under 1 M HCl. Over 1 h, cubic particles shrink and eventually dissolve completely. (b) Active trapping is achieved by introducing H_2O_2 as chemical fuel and TMAH to adjust pH around 9 for diffusiophoresis under blue light irradiation. Hematite catalyzes the decomposition of H_2O_2, and the chemical gradient formed drives fluorescent PS tracers toward the hematite. Tracers smaller than the pores collect in the cage, and entropic bottling ensures prolonged retention even after light is switched off. In this sample, the cages, created without the shrinking step, are expected to have fissures exceeding 200 nm. Scale bars: 3 μm.

Polymer-Coated TPM Cores. The TPM monomer oil is prehydrolyzed to form water-soluble species by vigorously stirring it in deionized water at a 1:10 v/v ratio until fully dissolved.

Colloidal cargoes such as hematite cubes and peanuts are prepared using a sol−gel method adapted from ref 36. Ammonia (6 wt%) is added to the suspension containing hematite particles, followed by a single addition of hydrolyzed TPM. The mixture is gently shaken using an orbital shaker for 55 min until no further growth is observed and then aged in ammonia for additional cross-linking.[27] Thinner coatings around cargo colloids can be achieved with higher ammonia concentrations and less TPM precursor.

A concentrated Pluronic F108 solution (5 wt%) is added to the core suspension to achieve a final concentration of approximately 0.05 wt%, well below the critical micellar concentration. The resulting polymer-coated cores are then purified through repeated centrifugation at 800 rpm for 30 min and resuspension in deionized water to eliminate any remaining free polymers in the solution. All particle syntheses are monitored using bright-field video microscopy, and in the case of solid particles, we additionally employ scanning electron microscopy.

In this study, the TPM cores typically exhibited a zeta potential of −40 mV, as measured with a Malvern Zetasizer NanoS. For a comprehensive electrophoretic characterization of the TPM colloidal system, readers are directed to ref 37.

Polymerized cores are created by exposing them to UV light for 25 min, using a RPR-100 RAYONET Photochemical Reactor equipped with sixteen 350 nm light bulbs. Darocur 1173 (Sigma-Aldrich) is introduced at a volume ratio of 1:1000 during this process.

Clusters Formation. PS satellites and liquid cores are combined in a 1000:1 number ratio. A standard protocol involves gently shaking equal volumes of satellites, cores, and a 60 mM NaCl stock solution. The caged cores are then purified through centrifugation or magnetic attraction (in the case of magnetic cargo) to remove excess shells and salt. The clusters can be UV-polymerized with Darocur 1173 and rinsed with THF to reveal satellite dimples.

The resulting clusters can be further utilized as new satellites for the formation of higher-order supraparticles (Figure S4).

Cages Recovery. Dichloromethane is added to a diluted suspension of clusters in a 1:10 v/v to allow swelling and fusion of the PS satellites. The mixture is incubated for approximately 10 s before applying vacuum to remove the volatile DCM. The optimal incubation depends on the PS cross-linking density and it is determined empirically. Colloidal cages are recovered by dissolving the TPM in ethanol and resuspended in deionized water for storage or further use. Structural characterization is performed by drying samples in air prior to SEM imaging (Carl Zeiss MERLIN Field Emission SEM).

Shrink-Packing. In a typical shrink-packing process 1 mL clusters' suspension is mixed with 5 mL 50% v/v ethanol solution to allow for TPM dissolution and corresponding core shrinkage. The mixture is incubated for 10 s before rapidly diluting it with pure water to lower the ethanol concentration below 5%. A gentle centrifugation is carried out to sediment the buckled clusters and set them back in deionized water. To fix and recover the shrink-packed cages we proceed as previously described for regular clusters.

Active Transmembrane Transport. Active transport experiments were performed on colloidal mixtures containing caged hematite particles and sulfate-functionalized fluorescent PS tracers (200 nm in diameter). Prior to light exposure, 65 μL of this suspension is mixed with 6.5 μL of 30 wt% H_2O_2 and 3.5 μL of 1 wt% tetramethylammonium hydroxide. The collodial system is then sealed inside a flat capillary and monitored using a Leica DMI3000 inverted microscope equipped with a 100× oil immersion objective and a digital camera (Hamamatsu ORCA Flash4.0 sCMOS). The cage is activated using blue light (λ = 430−490 nm) from an external light source (Leica EL6000) optically coupled to the microscope.

Delivery. The hematite cargo is slowly dissolved and released by addition of 1 M hydrochloric acid. The dissolution is monitored by bright-field microscopy.

■ ASSOCIATED CONTENT

Supporting Information

The Supporting Information is available free of charge at https://pubs.acs.org/doi/10.1021/acs.chemmater.3c01053.

Supplementary microscopy images and SEM images (PDF)

https://doi.org/10.1021/acs.chemmater.3c01053
Chem. Mater. 2023, 35, 6357−6363

Video showing active transmembrane transport (MP4)

AUTHOR INFORMATION

Corresponding Author

Stefano Sacanna − *New York University, New York, New York 10003, United States;* orcid.org/0000-0002-8399-3524; Email: s.sacanna@nyu.edu

Authors

Zhe Xu − *New York University, New York, New York 10003, United States;* orcid.org/0000-0002-8599-079X

Theodore Hueckel − *New York University, New York, New York 10003, United States;* Present Address: Department of Materials Science and Engineering, Massachusetts Institute of Technology, Cambridge, Massachusetts 02139, United States; orcid.org/0000-0002-4474-6280

William T. M. Irvine − *James Franck Institute, Enrico Fermi Institute, Department of Physics, University of Chicago, Chicago, Illinois 60637, United States;* orcid.org/0000-0002-4925-2060

Complete contact information is available at: https://pubs.acs.org/10.1021/acs.chemmater.3c01053

Notes

The authors declare no competing financial interest.

ACKNOWLEDGMENTS

This research was primarily supported by the U.S. Army Research Office under Award Number W911NF2010117.

REFERENCES

(1) Dingwall, C.; Laskey, R. The nuclear membrane. *Science* **1992**, *258*, 942−947.

(2) Dinsmore, A.; Hsu, M. F.; Nikolaides, M.; Marquez, M.; Bausch, A.; Weitz, D. Colloidosomes: selectively permeable capsules composed of colloidal particles. *Science* **2002**, *298*, 1006−1009.

(3) Velev, O.; Furusawa, K.; Nagayama, K. Assembly of latex particles by using emulsion droplets as templates. 1. Microstructured hollow spheres. *Langmuir* **1996**, *12*, 2374−2384.

(4) Datskos, P.; Polizos, G.; Bhandari, M.; Cullen, D.; Sharma, J. Colloidosome like structures: self-assembly of silica microrods. *RSC advances* **2016**, *6*, 26734−26737.

(5) Yue, X.; Liu, X.; Yan, N.; Jiang, W. Hierarchical Colloidosomes with a Highly Ordered and Oriented Arrangement of Gold Nanorods via Confined Assembly at the Emulsion Interface. *The Journal of Physical Chemistry C* **2020**, *124*, 20458−20468.

(6) Pang, M.; Cairns, A. J.; Liu, Y.; Belmabkhout, Y.; Zeng, H. C.; Eddaoudi, M. Synthesis and integration of Fe-soc-MOF cubes into colloidosomes via a single-step emulsion-based approach. *J. Am. Chem. Soc.* **2013**, *135*, 10234−10237.

(7) Wagner, C. S.; Fortini, A.; Hofmann, E.; Lunkenbein, T.; Schmidt, M.; Wittemann, A. Particle nanosomes with tailored silhouettes. *Soft Matter* **2012**, *8*, 1928−1933.

(8) Liu, D.; Zhou, F.; Li, C.; Zhang, T.; Zhang, H.; Cai, W.; Li, Y. Black Gold: Plasmonic Colloidosomes with Broadband Absorption Self-Assembled from Monodispersed Gold Nanospheres by Using a Reverse Emulsion System. *Angewandte Chemie International Edition* **2015**, *54*, 9596−9600.

(9) Xu, X.-W.; Zhang, X.-M.; Liu, C.; Yang, Y.-L.; Liu, J.-W.; Cong, H.-P.; Dong, C.-H.; Ren, X.-F.; Yu, S.-H. One-pot colloidal chemistry route to homogeneous and doped colloidosomes. *J. Am. Chem. Soc.* **2013**, *135*, 12928−12931.

(10) Kang, C.; Honciuc, A. Influence of geometries on the assembly of snowman-shaped Janus nanoparticles. *ACS nano* **2018**, *12*, 3741−3750.

(11) Jiang, H.; Sheng, Y.; Ngai, T. Pickering emulsions: Versatility of colloidal particles and recent applications. *Curr. Opin. Colloid Interface Sci.* **2020**, *49*, 1−15.

(12) Lee, D.; Weitz, D. A. Double emulsion-templated nanoparticle colloidosomes with selective permeability. *Adv. Mater.* **2008**, *20*, 3498−3503.

(13) Lee, D.; Weitz, D. A. Nonspherical colloidosomes with multiple compartments from double emulsions. *Small* **2009**, *5*, 1932−1935.

(14) Rossier-Miranda, F. J.; Schroën, K.; Boom, R. Microcapsule production by an hybrid colloidosome-layer-by-layer technique. *Food Hydrocolloids* **2012**, *27*, 119−125.

(15) Opdam, J.; Tuinier, R.; Hueckel, T.; Snoeren, T. J.; Sacanna, S. Selective colloidal bonds via polymer-mediated interactions. *Soft Matter* **2020**, *16*, 7438−7446.

(16) Harley, S.; Thompson, D. W.; Vincent, B. The adsorption of small particles onto larger particles of opposite charge direct electron microscope studies. *Colloids and surfaces* **1992**, *62*, 163−176.

(17) Schade, N. B.; Holmes-Cerfon, M. C.; Chen, E. R.; Aronzon, D.; Collins, J. W.; Fan, J. A.; Capasso, F.; Manoharan, V. N. Tetrahedral colloidal clusters from random parking of bidisperse spheres. *Physical review letters* **2013**, *110*, 148303.

(18) Eren, E. D.; Moradi, M.-A.; Friedrich, H.; de With, G. Building Reversible Nanoraspberries. *Nano letters* **2021**, *21*, 2232−2239.

(19) Yao, L.; Li, Q.; Guan, Y.; Zhu, X.; Zhang, Y. Tetrahedral, octahedral, and triangular dipyramidal microgel clusters with thermosensitivity fabricated from binary colloidal crystals template and thiol−ene reaction. *ACS Macro Letters* **2018**, *7*, 80−84.

(20) McGinley, J. T.; Jenkins, I.; Sinno, T.; Crocker, J. C. Assembling colloidal clusters using crystalline templates and reprogrammable DNA interactions. *Soft Matter* **2013**, *9*, 9119−9128.

(21) Demirörs, A. F.; Stiefelhagen, J. C.; Vissers, T.; Smallenburg, F.; Dijkstra, M.; Imhof, A.; Van Blaaderen, A. Long-ranged oppositely charged interactions for designing new types of colloidal clusters. *Physical Review X* **2015**, *5*, 021012.

(22) Van Der Wel, C.; Bhan, R. K.; Verweij, R. W.; Frijters, H. C.; Gong, Z.; Hollingsworth, A. D.; Sacanna, S.; Kraft, D. J. Preparation of colloidal organosilica spheres through spontaneous emulsification. *Langmuir* **2017**, *33*, 8174−8180.

(23) Youssef, M.; Hueckel, T.; Yi, G.-R.; Sacanna, S. Shape-shifting colloids via stimulated dewetting. *Nature Communications* **2016**, *7*, 12216.

(24) Thompson, K. L.; Williams, M.; Armes, S. P. Colloidosomes: synthesis, properties and applications. *Journal of colloid and interface science* **2015**, *447*, 217−228.

(25) Yang, Z.; Wei, J.; Sobolev, Y. I.; Grzybowski, B. A. Systems of mechanized and reactive droplets powered by multi-responsive surfactants. *Nature* **2018**, *553*, 313−318.

(26) Lu, J.; Liong, M.; Zink, J. I.; Tamanoi, F. Mesoporous silica nanoparticles as a delivery system for hydrophobic anticancer drugs. *small* **2007**, *3*, 1341−1346.

(27) Xu, Z.; Hueckel, T.; Irvine, W. T. M.; Sacanna, S. Transmembrane transport in inorganic colloidal cell-mimics. *Nature* **2021**, *597*, 220−224.

(28) Palacci, J.; Sacanna, S.; Kim, S.-H.; Yi, G.-R.; Pine, D. J.; Chaikin, P. M. Light-activated self-propelled colloids. *Philosophical Transactions of the Royal Society A: Mathematical, Physical and Engineering Sciences* **2014**, *372*, 20130372.

(29) Palacci, J.; Sacanna, S.; Steinberg, A. P.; Pine, D. J.; Chaikin, P. M. Living crystals of light-activated colloidal surfers. *Science* **2013**, *339*, 936−940.

(30) Cheng, K.-L.; Sheng, Y.-J.; Tsao, H.-K. Brownian escape and force-driven transport through entropic barriers: Particle size effect. *The Journal of chemical physics* **2008**, *129*, 184901.

(31) Grigoriev, I. V.; Makhnovskii, Y. A.; Berezhkovskii, A. M.; Zitserman, V. Y. Kinetics of escape through a small hole. *The Journal of chemical physics* **2002**, *116*, 9574−9577.

(32) Rodríguez-Arco, L.; Li, M.; Mann, S. Phagocytosis-inspired behaviour in synthetic protocell communities of compartmentalized colloidal objects. *Nature materials* **2017**, *16*, 857−863.

(33) Cayre, O. J.; Hitchcock, J.; Manga, M. S.; Fincham, S.; Simoes, A.; Williams, R. A.; Biggs, S. pH-responsive colloidosomes and their use for controlling release. *Soft Matter* **2012**, *8*, 4717−4724.
(34) Sander, J. S.; Studart, A. R. Monodisperse functional colloidosomes with tailored nanoparticle shells. *Langmuir* **2011**, *27*, 3301−3307.
(35) Hester, J.; Olugebefola, S.; Mayes, A. Preparation of pH-responsive polymer membranes by self-organization. *J. Membr. Sci.* **2002**, *208*, 375−388.
(36) Sugimoto, T.; Khan, M. M.; Muramatsu, A. Preparation of monodisperse peanut-type α-Fe2O3 particles from condensed ferric hydroxide gel. *Colloids and Surfaces A: Physicochemical and Engineering Aspects* **1993**, *70*, 167−169.
(37) Youssef, M.; Morin, A.; Aubret, A.; Sacanna, S.; Palacci, J. Rapid characterization of neutral polymer brush with a conventional zetameter and a variable pinch of salt. *Soft Matter* **2020**, *16*, 4274−4282.

https://doi.org/10.1021/acs.chemmater.3c01053
Chem. Mater. 2023, 35, 6357−6363